Journal of Thermal Analysis and Calorimetry, Vol. 69 (2002) 985–996

ORIENTATIONAL ORDERING OF PYRIDINIUM ION IN ITS TETRABROMOAURATE(III) SALT
Intermediate situation between Schottky anomaly and phase transition

H. Fujimori[1*], *T. Asaji*[1], *M. Hanaya*[2] *and M. Oguni*[3]

[1]Department of Chemistry, College of Humanities and Sciences, Nihon University, Sakurajosui, Setagaya-ku, Tokyo 156-8550, Japan
[2]Department of Materials Chemistry, Faculty of Engineering, Gunma University, Tenjin-cho 1-5-1, Kiryu, Gunma 376-8515, Japan
[3]Department of Chemistry, Graduate School of Science and Engineering, Tokyo Institute of Technology, Ookayama, Meguro-ku, Tokyo 152-8551, Japan

Abstract

Heat capacity and dielectric measurements of crystalline pyridinium tetrabromoaurate(III), (pyH)$AuBr_4$, were carried out in the temperature ranges of 13 to 300 K and 30 to 160 K, respectively. A phase transition, due to the orientational ordering of pyridinium ions, was found at 99.9 K. A glass transition, due to freezing-in of the reorientational motion of pyridinium ions, was found at around 60 K. An anomaly showing the intermediate situation between Schottky effect and phase transition was found with the heat-capacity peak at around 260 K.

Keywords: cooperative effect, dielectric constant, glass transition, heat capacity, phase transition, pyridinium ion, pyridinium tetrabromoaurate(III), Schottky effect

Introduction

Pyridinium tetrahalogenoaurate(III) ((pyH)AuX_4, *X*=Cl, Br) consists of planar pyridinium cations and square-planar complex anions of tetrahalogenoaurate(III), and the space group of the crystal structure was assigned to be *C*2/*m* [1, 2]. The nitrogen atom in each pyridinium ion was found by X-ray diffraction experiment to be disordered among six carbon/nitrogen sites at room temperature [2], and the disorder was indicated to be dynamic, but not static, with respect to the orientation of pyridinium ion about its pseudohexad axis C_6' by ^{1}H NMR measurements [1, 3]. Although the orientation of pyridinium ions is to be ordered at low temperatures, the ordering phase-transition and the structure of the ordered phase have not been found yet. Ito *et al*. [1] observed the anomalous behavior of the second-moment M_2 in the

* Author for correspondence: E-mail: fujimori@chs.nihon-u.ac.jp

1418–2874/2002/ $ 5.00

Akadémiai Kiadó, Budapest
Kluwer Academic Publishers, Dordrecht

^{1}H NMR absorption; M_2 changed from the dynamically disordered to ordered values over an extremely wide temperature range. They explained it by introducing non-equivalent potential wells for the reorientational motion about C'_6 axis of pyridinium ion [1]. In the present study, heat capacity and dielectric measurements of pyridinium tetrabromoaurate(III) crystals were carried out to get the information about the ordering process of pyridinium ions with decreasing temperature.

Experimental

(pyH)$AuBr_4$ used for the NMR/NQR measurements [1] was employed in the present thermal and dielectric measurements. It was synthesized by mixing pyridine dissolved in hydrobromic acid and $HAuBr_4$, which was obtained by dissolving a gold wire in a conc. hydrobromic acid containing bromine, and was purified by recrystallization from 4 mol dm^{-3} hydrobromic acid solution. The result of an elemental analysis is reported as follows [1]: Calculated: C, 10.06%; H, 1.01%; Br, 53.56%, Found: C, 10.0%; H, 1.0%; Br, 53.4%.

The sample was loaded into a calorimeter cell under a helium atmosphere at 105 Pa. The mass of the sample employed was found to be 7.5207 g (corresponding to 12.604 mmol). The heat capacities were measured in the temperature range between 13 and 300 K by using an adiabatic calorimeter. A platinum resistance thermometer (Minco Products S1059, USA), which had a nominal resistance of 100 ohm at 273.16 K, was used after the temperature scale was transferred from the other thermometer calibrated on the ITS-90. The imprecision and inaccuracy of the measurements with the apparatus were estimated previously to be less than 0.04 and 0.4%, respectively [4].

The dielectric measurements were carried out for the pressed polycrystalline pellet (~1 mm thick and 10 mm in diameter) with silver-paste electrodes painted on the surfaces. The measurements were carried out on heating the sample from 30 to 160 K at a rate of 0.1 K min^{-1} by using an EG&G DSP7260 lock-in amplifier in the frequency range between 1 and 10^5 Hz [5, 6]. An oscillating electric voltage applied to the cell was set at 1 V.

Results and discussion

Heat capacity measurements

Experimental molar heat capacities of (pyH)$AuBr_4$ at constant pressure $C_{p,m}$ are tabulated in Table 1 and are shown graphically in Fig. 1. The results were obtained for the sample precooled at a rate of 5 mK min^{-1} in the temperature range from 68 to 55 K. No anomalous temperature drift and temperature hysteresis effect were observed except in the temperature range between 50 and 70 K. Figure 2 shows the temperature dependence of the rates of spontaneous temperature drifts observed around 60 K in the heat capacity measurements on heating. In the sample cooled rapidly (4 K min^{-1}) prior to the measurements, spontaneous exothermic effect appeared around 60 K. In the sample cooled slowly (5 mK min^{-1}), on the other hand, spontaneous endothermic

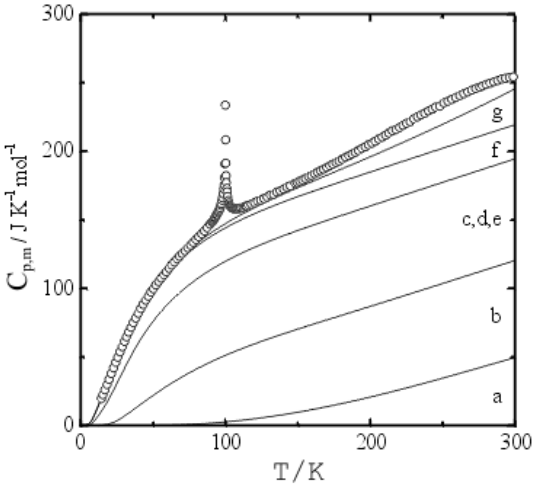

Fig. 1 Molar heat capacities of pyridinium tetrabromoaurate(III), (pyH)$AuBr_4$, and separation of the heat capacities into the contributions from different degrees of freedom: a – intra-molecular vibrations of pyridinium ion; b – those of tetrabromoaurate ion; c – rotational vibrations of pyridinium ion; d – those of tetrabromoaurate ion; e – a part of lattice vibrations calculated by using the Einstein's function; f – the other part of lattice vibrations calculated by the Debye's function; g – C_p–C_v correction. See text for the detail

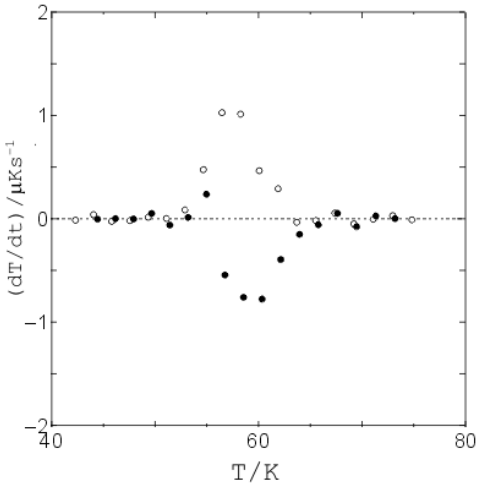

Fig. 2 Spontaneous temperature-drift rates after each energy input: open and solid circles are of the samples cooled at a rate of 4 K min^{-1} and at 5 mK min^{-1} prior to the measurements, respectively. The 'spontaneous' means that the rate derived was estimated by subtracting the rate of small stationary drift from the observed one

effect appeared around 60 K. This dependence on the thermal history of the sample is characteristic of a glass transition in the crystalline phase [7, 8]. The glass transition temperature was determined to be 60 K according to the empirical relation [9, 10]. The heat capacity jump associated with the glass transition will be estimated later.

Three anomalies were found; a phase transition at 99.9 K, a glass transition at 60 K, and a heat capacity peak (at around 260 K) characteristic of Schottky anomaly. Excess part of heat capacity was derived by subtracting normal part from the observed value. The normal heat capacity was determined as composed of the contributions from intra-ionic vibrations of pyridinium ion (a, 30 degrees of freedom, hereafter abbreviated with only the number of degrees in parenthesis), those of tetrabromoaurate ion (b, 9), rotational vibrations of pyridinium and tetrabromoaurate ion (c, 3 and d, 3, respectively), lattice vibrations of optical mode (e, 3), lattice vibrations of acoustic mode (f, 3), and a C_p–C_v correction term (g). The contributions of a, b, c, d and e were estimated by using the Einstein function, and that of f by using the Debye function. The C_p–C_v correction term is often approximated by the expression,

$$C_p - C_v = \frac{\alpha^2 V_m T}{\beta} \approx A C_p^2 T, \tag{1}$$

where α, β, and V_m are the thermal expansivity, isothermal compressibility, and molar volume, respectively, and A is some compound-dependent constant [11]. Since neither α nor β have been known at all, the approximate equation was employed. The intramolecular-vibrational frequencies obtained by IR and Raman measurements of (pyH)Br [12] and $AuBr_4^-$ ions [13] were used for those of pyridinium and tetrabromoaurate ions, respectively. With three Einstein temperatures θ_E's for the rotational vibrations of the cation and anion and for the optical lattice vibrations, Debye temperature θ_D for the acoustical lattice vibrations and A as adjustable parameters, the observed heat capacities in the temperature range between 13 and 50 K (below the glass transition temperature) were fitted. The derived parameters were θ_E=45, 119, and 119 K, θ_D=75 K and A=1.45·10^{-6} J^{-1} mol, respectively. The respective contributions to the heat capacity are depicted in Fig. 1 as the portions divided by full curves.

The anomalous heat capacities derived are plotted in Fig. 3. The broad heat-capacity peak is found clearly to exist at around 260 K. The anomaly was analyzed based on a kind of Schottky effect. The Schottky heat capacity for a two-level system is given by

$$C_{Sch} = \frac{\Delta\varepsilon_0^2}{RT^2} \frac{g_1}{g_0} \frac{\exp(-\Delta\varepsilon_0/RT)}{[1+(g_1/g_0)\exp(-\Delta\varepsilon_0/RT)]^2} \tag{2}$$

where g_0, g_1 and $\Delta\varepsilon_0$ are degeneracies of the ground and excited states, respectively, and a molar energy separation between the two states [14]. Since Ito *et al*. [1] concluded from ^{1}H NMR experiments that there exist high and low energy levels with the degeneracies of 4 and 2, respectively, for the orientations about C_6' axis of pyridinium ion [1], the g_1/g_0 was assumed to be 2. Then the maximum heat capacity occurs at T_m=0.377($\Delta\varepsilon_0/R$). Since T_m appeared at about 264 K in the present case, the Schottky

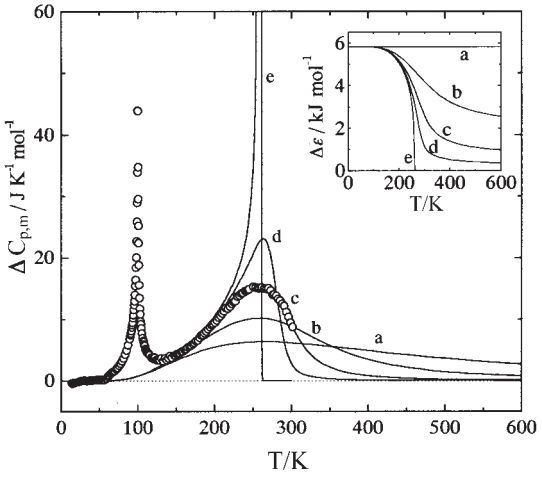

Fig. 3 Excess heat capacities derived by subtracting the normal part from the observed values. Solid lines represent the heat capacity curves, as given by Eq. (5), calculated by assuming the Schottky anomaly including the cooperative effect with parameters of $\Delta\varepsilon_0$=5.82 kJ mol^{-1} and E: a – E=0 kJ mol^{-1}; b – 4 kJ mol^{-1}; c – 5.2 kJ mol^{-1}; d – 5.6 kJ mol^{-1}; e – 5.82 kJ mol^{-1}. The inset shows the estimated temperature dependence of the $\Delta\varepsilon$. The curve e corresponds to the case of a phase transition given by a Potts model with degeneracies 1 and 2 in the ground and excited states, respectively. See text for the detail

heat capacity was first calculated using $\Delta\varepsilon_0$=5.82 kJ mol^{-1} as represented by solid line (a) in Fig. 3. The calculated heat capacities, however, do not agree with the observed ones; the calculated values are lower in the region of the heat-capacity peak and higher on the high temperature side. The reason may be that the Schottky effect includes no cooperative effect. We have introduced a kind of cooperative effect through a molecular-field approximation as follows. The energy separation $\Delta\varepsilon$ is assumed to be temperature-dependent through an expression

$$\Delta\varepsilon=\Delta\varepsilon_0-\frac{3}{2}E(1-f) \tag{3}$$

Here, E is a parameter representing the cooperative effect, and f is the occupation fraction in the ground state given by

$$f=\frac{1}{1+2\exp(-\Delta\varepsilon/RT)} \tag{4}$$

At 0 K f=1 and $\Delta\varepsilon=\Delta\varepsilon_0$, and at infinite temperature f=1/3 and $\Delta\varepsilon=\Delta\varepsilon_0-E$ ($=\Delta\varepsilon\,\infty$). Heat capacity of Schottky type for the two-level system with g_1/g_0=2 was calculated by use of thermodynamic equations of

$S=-R\sum_i(p_i\ln p_i)$ and $C=T(\partial S/\partial T)_v$,

which relate heat capacity C, entropy S, and probability p_i of each microscopic state. The result can be written as

$$C=\frac{2R\Delta\varepsilon f(1-f)\{\ln 2+\ln[f/(1-f)]\}}{2RT-3Ef(1-f)} \quad (5)$$

Solid lines in Fig. 3 show the heat capacities of the Schottky anomaly calculated for $\Delta\varepsilon_0$=5.82 kJ mol^{-1} and different E's. The cooperative effect increases with increasing E, leading to a phase transition expressed by Potts model when $\Delta\varepsilon_0=E$. The phase transition appears as of a first order (solid line (e) in Fig. 3). In the present case, the observed heat capacities in the temperature range from 150 to 300 K were fitted with $\Delta\varepsilon_0$ and E as adjustable parameters. The parameters $\Delta\varepsilon_0$ and E derived as giving the best fit were 5.82 and 5.20 kJ mol^{-1}, respectively, and the heat capacity curve derived is drawn with solid line (c) in Fig. 3. The anomaly showing the peak at around 260 K looks completely fitted by the Schottky anomaly with the cooperative effect. The temperature dependence of the $\Delta\varepsilon$ derived is shown in the upper-right inset of Fig. 3.

The $\Delta\varepsilon$ derived from the NMR measurements was 4.8 kJ mol^{-1} [1]. It corresponds with the value at 220 K derived by the above calculation. Since the NMR measurements were carried out in the temperature range between 100 and 300 K, and the $\Delta\varepsilon$ was assumed to be constant in the measurement temperature range, the $\Delta\varepsilon$ from NMR should be the mean value of the energy separation. Therefore, it seems that the agreement between the NMR and the present studies is fairly good.

It is interesting to consider why there remains 0.62 kJ mol^{-1} of energy separation even at the high temperature limit and the occurrence of the phase transition is interrupted. In view of the fact that the dispersion force with the other constituent atoms is essentially same between N–H and C–H groups, a kind of hydrogen-bonding interaction of N^+–H···Cl^- would play the role to stabilize somehow the ground-state orientations. The observation that the crystal structure is in the monoclinic system with $\beta\neq90°$ so that the N–H group in the ground state can come close to chloride ions than otherwise would be interrelated with the present finding.

The excess heat capacities derived by subtracting the normal part and the Schottky anomaly including the cooperative effect from the observed values are shown in Fig. 4. The upper-left inset shows the excess heat capacities on an enlarged scale in the glass transition region. The dashed line was drawn as a guide for eyes. The molar heat capacity jump associated with the crystalline glass transition was estimated at 60 K to be 1.0 J K^{-1} mol^{-1} corresponding to 0.9% of the total heat capacity.

A large anomaly in the excess heat capacities was observed with a peak at around 100 K without any anomalous temperature drift. This indicates that the phase transition is of the second order. The transition point T_c was determined to be 99.9 K as the temperature of the heat capacity peak. The transition enthalpy and entropy were estimated to be 409 J mol^{-1} and 4.29 J K^{-1} mol^{-1} , respectively, from the excess heat capacities. Since the reorientational motion of pyridinium ion is in the frozen-in state below the glass transition temperature, the excess heat capacities below 65 K

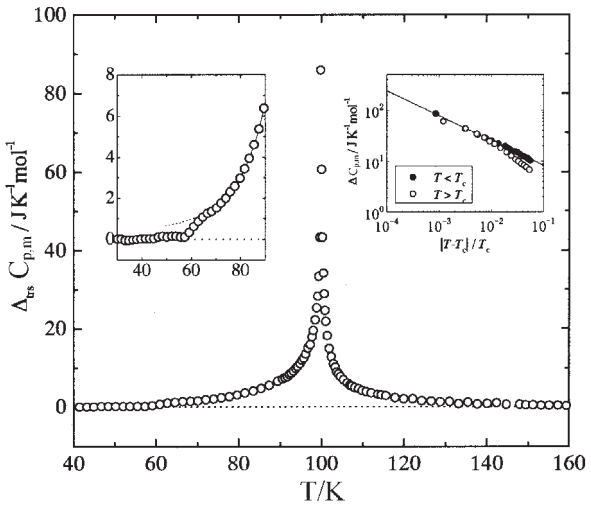

Fig. 4 Excess heat capacities derived by subtracting the normal part and the Schottky anomaly with cooperative effect from the observed values. The inset in the upper left shows the excess heat capacities on an enlarged scale in the glass transition region, and that in the upper right the usual logarithmic plot of the excess heat capacity around the critical temperature T_c

were estimated and included into the transition entropy. Assuming that the heat capacity is zero at 0 K, the data in the temperature range from 65 to 75 K were fitted by a polynomial function. The estimated transition entropy below 65 K was found to be 0.27 J K^{-1} mol^{-1}. This corresponds to the residual entropy due to the glass transition. The total transition entropy including the residual one amounts to 4.56 J K^{-1} mol^{-1} corresponding to Rln1.73 close to Rln2. This transition was therefore interpreted reasonably as originating from the ordering of pyridinium ions between the sites related by 180° rotation about the axis perpendicular to the molecular plane (the pseudodiad axis C_2') [1].

It is noticed that the excess heat capacity curve exhibits long tails over wide temperature ranges on the both sides of the transition temperature, and that the shape of the tails is quite symmetrical (see Fig. 4). This indicates that the inter-ionic interaction governing the orientations of the pyridinium ions is two-dimensional in character. This would be interrelated with the layer structure of (pyH)$AuBr_4$ crystal similar to (pyH)$AuCl_4$ [1, 2]. The upper-right inset of Fig. 4 shows the logarithmic plot of the excess heat capacities in the temperature range close to the critical point T_c. The critical index of the excess heat capacities was estimated to be 0.49 (≈0.5) by fitting the data in the region of $-0.04<(T-T_c)/T_c<0$. The fitted result is shown with a solid line in the figure. In the region of $T>T_c$, the excess heat capacities are not on the straight line and rather smaller than that. This indicates that the inter-ionic interaction is not completely two-dimensional, but includes slightly a three-dimensional component.

Table 1 Molar heat capacities of pyridinium tetrabromoaurate(III), $(pyH)AuBr_4$

T/K	$C_{p,m}$/ J K^{-1}mol^{-1}	T/K	$C_{p,m}$/ J K^{-1}mol^{-1}	T/K	$C_{p,m}$/ J K^{-1}mol^{-1}	T/K	$C_{p,m}$/ J K^{-1}mol^{-1}
14.21	19.63	87.40	145.0	108.99	158.9	196.47	203.7
15.35	22.60	89.38	147.5	109.90	159.0	198.78	205.1
16.72	26.29	90.60	149.0	110.80	159.3	201.10	206.3
18.15	30.16	91.20	149.7	112.05	159.7	203.44	207.7
19.56	33.96	91.72	150.5	113.62	160.3	205.79	209.2
21.11	38.15	92.23	151.4	114.51	160.7	208.15	210.6
22.71	42.42	92.74	152.1	115.65	161.1	210.53	212.2
24.20	46.40	93.24	152.9	117.79	161.9	212.92	213.7
25.70	50.35	93.75	154.0	119.95	162.9	215.33	215.3
27.19	54.23	94.25	154.8	122.12	164.2	217.74	216.3
28.68	58.04	94.75	156.0	124.31	164.9	220.18	217.8
30.17	61.75	95.25	157.2	126.51	166.1	222.62	219.5
31.66	65.31	95.74	158.0	128.72	167.1	225.08	220.9
33.16	68.72	96.23	159.5	130.96	168.5	227.55	222.3
34.70	72.18	96.72	161.3	133.21	169.1	230.04	224.2
36.30	75.64	97.21	162.5	135.48	170.7	232.54	225.6
37.97	79.11	97.70	164.9	137.76	171.5	235.05	227.1
39.70	82.57	98.04	166.7	140.06	172.9	237.57	228.5
41.44	85.91	98.52	169.8	142.37	174.4	240.11	230.0
43.18	89.07	98.88	173.1	144.71	175.2	242.67	231.4
44.93	92.12	99.12	176.3	147.96	177.0	245.23	232.8
46.68	95.11	99.35	181.5	149.44	177.7	250.85	235.9
48.45	97.97	99.59	191.7	151.17	178.6	253.55	237.1
50.22	100.6	99.81	234.7	153.15	179.6	256.27	238.3
51.99	103.3	100.02	209.3	155.18	180.7	259.00	239.6
53.78	105.7	100.23	192.1	157.24	181.8	261.75	241.0
55.56	108.1	100.43	183.0	159.31	182.8	264.51	242.2
57.36	110.5	100.64	177.9	161.39	184.0	267.28	243.5
59.16	112.9	100.84	173.7	163.48	185.1	270.06	245.0
60.97	115.4	101.06	171.1	165.59	186.3	272.86	245.9
62.79	117.7	101.41	167.6	167.70	187.3	275.67	246.7
64.62	120.0	101.88	164.7	169.83	188.5	277.43	247.6
66.45	122.1	102.34	162.8	171.98	189.7	280.05	248.6
68.30	124.1	102.81	161.4	174.14	190.9	282.70	249.5

Table 1 Continued

T/K	$C_{p,m}$/ J K^{-1}mol^{-1}	T/K	$C_{p,m}$/ J K^{-1}mol^{-1}	T/K	$C_{p,m}$/ J K^{-1}mol^{-1}	T/K	$C_{p,m}$/ J K^{-1}mol^{-1}
70.15	126.2	103.27	160.7	176.31	192.1	285.36	250.5
72.02	128.2	103.73	159.9	178.49	193.2	288.03	251.3
73.90	130.2	104.20	159.7	180.69	194.6	290.72	252.3
75.79	132.3	104.66	159.2	182.91	196.0	293.42	252.7
77.69	134.2	105.35	158.9	185.13	197.1	296.14	253.2
79.60	136.3	106.26	158.7	187.37	198.4	298.87	253.7
81.53	138.4	106.94	158.6	189.63	199.7	301.62	254.4
83.47	140.5	107.40	158.6	191.89	201.0		
85.43	142.7	108.08	158.7	194.18	202.4		

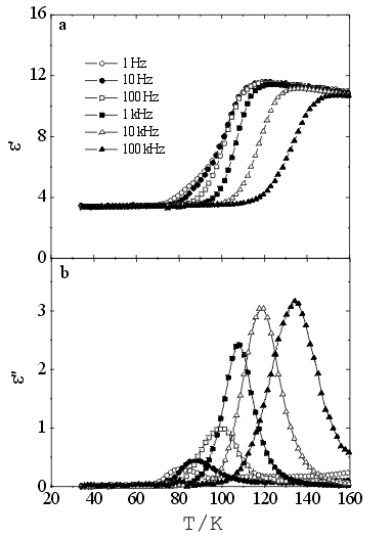

Fig. 5 The real (a) and imaginary (b) parts of dielectric constant of (pyH)$AuBr_4$ as functions of temperature and frequency

Dielectric measurements

Figure 5 shows the temperature dependence of the real and imaginary parts, ε′ and ε″, respectively, of the dielectric constant observed in (pyH)$AuBr_4$. The dielectric dispersion was observed in the temperature range of 70–160 K. The origin is considered to be the reorientational motion of pyridinium ions. Two things are pointed out with respect to the phase transition at 99.9 K: One is, in view that there was no dielectric divergence observed in the ε′, the phase transition does not lead to a ferroelectric phase at low temperatures. The other is, the ε′ values at 1, 10, and 100 Hz decrease together

around 100 K in association with the phase transition, and the ε″ peaks at those frequencies become much small as compared with the peaks (appearing above 100 K) at higher frequencies. This confirms that the phase transition is associated with the orientational ordering of pyridinium ions.

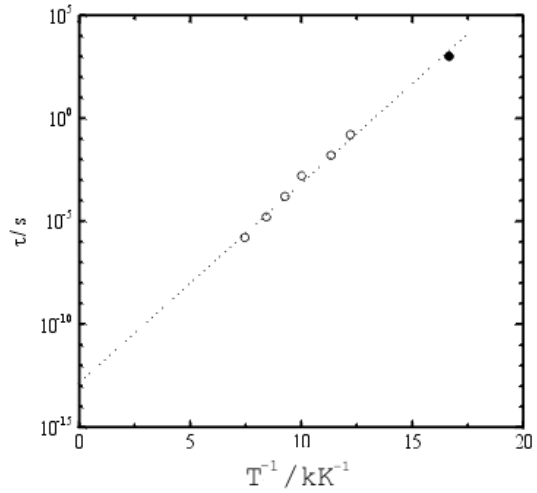

Fig. 6 Arrhenius plot of the relaxation times for the reorientation of pyridinium ion about its pseudodiad axis C_2': open circles, by dielectric measurements; solid circle, by calorimetry

The relaxation times are shown as an Arrhenius plot in Fig. 6 together with that obtained by the above calorimetric measurement; The glass transition point by the adiabatic calorimetry is given as the temperature at which the relaxation time becomes 10^3 s. All the relaxation times derived by both methods can be connected with a straight line as shown with the dashed line in the figure. This indicates that the dielectric dispersion, glass transition, and phase transition are all related to the same reorientational motion of the pyridinium ions, and that the activation energy for the motion does not change even through the phase transition. Considering that the transition entropy is nearly *R*ln2, the motion is judged to be the reorientation of pyridinium ion about its pseudodiad axis C_2'. The activation energy of the motion is found to be 18 kJ mol^{-1} according to the Arrhenius equation adapted to the dashed line in Fig. 6. The activation energy, however, does not agree very well with the activation energy 22 kJ mol^{-1} derived from NMR study [1] for the cationic reorientation from a stable to a metastable orientation. This may be partly due to that the dielectric relaxation data were analyzed by assuming a single relaxation time although really two independent relaxation times should be introduced for the pyridinium motion in the nonequivalent potential wells consisting of two deep and four shallow wells [1, 15].

Conclusions

Calorimetric and dielectric studies of a (pyH)$AuBr_4$ crystal were carried out, and two ordering processes of pyridinium ion were found. One is the orientational ordering of the ion about the pseudodiad axis C'_2, and was observed as the second-order phase transition at 99.9 K. The activation energy for the associated reorientation was estimated to be 18 kJ mol^{-1}. This motion was frozen in through a glass transition at 60 K. The other is the orientational ordering of the ion about the pseudohexad axis C'_6, and the heat capacity curve due to the ordering was understood as reproduced by a modified Schottky anomaly with a cooperative effect. The curve showed its maximum at around 260 K. The energy separation between the two energy levels was interpreted to depend on temperature, and was estimated to be 5.82 kJ mol^{-1} at 0 K and 0.62 kJ mol^{-1} at infinite temperature. The presence of the energy difference of 0.62 kJ mol^{-1} even in the highly disordered state should be understood consistently with the crystal structure, and it is intriguing to clarify the microscopic reason why the occurrence of the phase transition is interrupted. The behavior is also interesting in the comparison with those in (pyH)I and (pyH)PF_6 where the structures of the anions are not planar and the ordering proceeds in one step through a phase transition [16].

* * *

This work was partly supported by the following grants: Cooperative Research Grant from the Institute of Natural Sciences, Nihon University; a Grant from College of Humanities and Sciences, Nihon University; a Grant from the Ministry of Education, Science, Sports and Culture to promote advanced scientific research; Saneyoshi Scientific Research Grant from Saneyoshi Scholarship Foundation.

References

1 Y. Ito, T. Asaji, R. Ikeda and D. Nakamura, Ber. Bunsenges. Phys. Chem., 92 (1988) 885.
2 H.-N. Adams and J. Strähle, Z. Anorg. Allg. Chem., 485 (1982) 65.
3 A. Ishikawa, Y. Ito, K. Horiuchi, T. Asaji and D. Nakamura, J. Mol. Struct., 192 (1989) 221.
4 K. Kobashi, T. Kyomen and M. Oguni, J. Phys. Chem. Solids, 59 (1998) 667.
5 M. Hanaya, M. Nomoto, T. Miura and M. Oguni, Solid State Commun., 115 (2000) 57.
6 B. G. Kim and J. J. Kim, Phys. Rev., B55 (1997) 5558.
7 H. Suga and S. Seki, J. Non-Cryst. Solids, 16 (1974) 171.
8 H. Suga and S. Seki, Faraday Discussions, 69 (1980) 221.
9 H. Fujimori and M. Oguni, J. Phys. Chem. Solids, 54 (1993) 271.
10 H. Fujimori and M. Oguni, J. Phys. Chem. Solids, 54 (1993) 607.
11 V. W. Nernst and F. A. Lindemann, Z. Elektrochem., 18 (1911) 817.
12 R. Foglizzo and A. Novak, J. Chim. Phys., 66 (1969) 1539; J. Chem. Phys., 50 (1969) 5366.
13 K. Nakamoto, Infrared Spectra of Inorganic and Coordination Compounds, 2nd Ed., Wiley-Interscience, New York 1970, p. 115.
14 E. S. R. Gopal, Specific Heats at Low Temperatures, Plenum Press, New York 1966, p. 102.

15 The orientations of the pyridinium ion are described as located in the pseudohexad potential field [1, 2]. In fact, the reorientation of the ion about the C_2' axis proceeds through surmounting two different potential barriers.
16 M. Hanaya, N. Ohta and M. Oguni, J. Phys. Chem. Solids, 54 (1993) 263.